

# Persistent supersolid phase of hard-core bosons on the triangular lattice

Dariusz Heidarian and Kedar Damle

*Department of Theoretical Physics, Tata Institute of Fundamental Research,  
Homi Bhabha Road, Colaba, Mumbai 400005, India*

(Dated: May 10, 2005)

We study hard-core bosons with unfrustrated hopping ( $t$ ) and nearest neighbour repulsion ( $U$ ) on the triangular lattice. At half-filling, the system undergoes a zero temperature ( $T$ ) quantum phase transition from a superfluid phase at small  $U$  to a supersolid at  $U_c \approx 4.45$  in units of  $2t$ . This supersolid phase breaks the lattice translation symmetry in a characteristic  $\sqrt{3} \times \sqrt{3}$  pattern, and is remarkably stable—indeed, a smooth extrapolation of our results indicates that the supersolid phase persists for arbitrarily large  $U/t$ .

PACS numbers: 75.10.Jm 05.30.Jp 71.27.+a

*Introduction:* The observation of strongly correlated Mott insulating states and  $T = 0$  superfluid-insulator transitions of ultracold bosonic atoms subjected to optical lattice potentials<sup>1</sup> has led to a great deal of interest in strongly correlated lattice systems that can be realized in such experiments.<sup>2,3</sup> The recent observation of a supersolid phase in Helium<sup>4</sup> leads, in this context, to a natural question: Can the lattice analog of this, namely a superfluid phase that simultaneously breaks lattice translation symmetry, be seen in atom-trap experiments?

One class of promising candidates are systems which are superfluid when interactions are weak, but form insulators with spatial symmetry breaking when interactions are strong: In terms of conventional Landau theory, a direct transition between these two states is generically either first order, or pre-empted by an intermediate supersolid phase with both order parameters nonzero; both types of behaviour are known to occur in specific lattice models.<sup>5,6,7</sup> Moreover, as has been shown recently by Senthil *et al.*,<sup>8</sup> conventional Landau theory can fail in certain situations in which quantum mechanical Berry phase effects produce a direct second-order phase transition, thereby ruling out an intermediate supersolid phase. When such a transition occurs,<sup>9,10</sup> it is associated with quasi-particle fractionalization and deconfinement, and this alternative to an intermediate supersolid phase is thus interesting in its own right.

Bosons on the triangular lattice with on-site repulsion  $V$ , repulsive nearest neighbour interaction  $U$ , and unfrustrated hopping ( $t$ ) provide a particularly interesting example in this context since the structure of interactions is simple enough that it can be realized in atom-trap experiments.<sup>2,11</sup> In the hard-core  $V \rightarrow \infty$  limit (which is also experimentally feasible<sup>2,11</sup>) this maps to a system of  $S = 1/2$  spins ( $S_i^z = n_i - 1/2$  where  $n_i$  is the boson number at site  $i$ ) with antiferromagnetic exchange  $J^z = U$  between the  $z$  components of neighbouring spins, ferromagnetic exchange  $J_\perp = 2t$  between their  $x$  and  $y$  components, and magnetic field in the  $z$  direction equal to the chemical potential  $\mu$ . It is this hard-core limit we consider in some detail below at zero chemical potential.

Clearly, the ground-state in the limit  $U/t \rightarrow 0$  must

be a featureless superfluid. On the other hand, the interaction energy  $U$  dominates in the  $U/t \rightarrow \infty$  limit and leads to frustration since it is impossible to have all pairs of neighbouring spins pointing anti-parallel to each other along the  $z$  axis on the triangular lattice. The ground state in this limit is thus expected to live entirely in the highly degenerate minimally frustrated subspace of configurations with precisely one frustrated bond (parallel spins) per triangle, and is selected by the dynamics associated with the hopping term  $t$ . The minimally frustrated subspace can be conveniently represented by noting that each state in this subspace corresponds to a perfect dimer cover of the dual hexagonal lattice (with every frustrated bond on the triangular lattice mapping to a dimer placed on the dual link perpendicular to the bond in question). In this language, the effective Hamiltonian in the  $U/t \rightarrow \infty$  limit is then a quantum dimer model with a ring-exchange term that operates on each pair of adjacent hexagons of the dual lattice (see Fig. 1).

Quantum dimer models with ring-exchange on individual plaquettes of two dimensional bipartite lattices quite generally have crystalline ground states in which the spatial arrangement of dimers breaks lattice symmetry.<sup>12,13</sup> In our problem, a wavefunction that gains kinetic energy from the double-hexagon ring exchange process on a maximal set of *independently flippable* hexagon pairs (see Fig. 1) provides a similar candidate lattice symmetry breaking insulating state at large  $U/t$  (see Fig. 1). Note however that this analogy to simpler quantum dimer models misses the important  $U(1)$  symmetry associated with charge conservation. Alternatively, one can focus on this  $U(1)$  symmetry at large  $U/t$  by thinking in terms of superfluid wavefunctions projected into the minimally frustrated subspace: Clearly, superfluidity can survive in such a projected state since the minimally frustrated manifold admits considerable charge fluctuations, and such wavefunctions also provide substantial kinetic energy gain.<sup>14</sup> The breaking of lattice translation symmetry that seems natural by analogy to the simpler quantum dimer models then motivates a large- $U$  variational ground state obtained by projecting a supersolid wavefunction.<sup>14</sup> This suggests that the ‘intermediate’ super-

solid phase of Landau theory may, in fact, persist to large  $U$  in this case (another argument for a supersolid was given in Ref. 15).

While these considerations are not definitive, they do at least emphasize that the behavior of this system at intermediate and large  $U$  presents very interesting possibilities, and a detailed numerical study is one way to decide between them. In the present work, we use Quantum Monte-Carlo (QMC) methods to perform such a numerical study. Our results for the different  $T = 0$  phases are shown in Fig. 1. To summarize, we find that the superfluid at small  $U$  undergoes a transition to a *supersolid* phase at  $U_c \approx 4.45$  in units of  $2t$ . This supersolid phase breaks lattice translation symmetry in a characteristic  $\sqrt{3} \times \sqrt{3}$  pattern shown in Fig. 1, and appears to be indeed stable for arbitrarily large values of  $U/t$  (albeit with progressively smaller superfluid density).

*Model and method:* Our Hamiltonian reads

$$H = \sum_{\langle ij \rangle} [U(n_i - 1/2)(n_j - 1/2) - t(b_i^\dagger b_j + b_i b_j^\dagger)] + \sum_i [V(n_i - 1/2)^2 - \mu n_i], \quad (1)$$

where  $\langle ij \rangle$  refer to nearest neighbour links of the two-dimensional triangular lattice,  $n_i$  is the particle number at site  $i$ , and  $b_i^\dagger$  is the boson creation operator at site  $i$ . In this work, we take the limit  $V \rightarrow \infty$  to enforce the hardcore constraint, thereby mapping it to the  $S = 1/2$  spin model as mentioned earlier, set  $t$  to  $1/2$ , and take  $\mu = 0$ . We use the well-documented stochastic series expansion (SSE) QMC method<sup>16,17,18</sup> which efficiently samples the high-temperature expansion of the grand-canonical partition function. (At large values of  $U/t$ , some modifications to the standard algorithm are necessary, and these will be discussed separately<sup>19</sup>).

Most of our data is on  $L \times L$  samples with periodic boundary conditions and  $L$  a multiple of six ranging from 12 to 48 at inverse temperatures  $\beta$  ranging from 10 to 30. Our choice of boundary conditions and aspect ratio ensures that all the lattice symmetries are preserved after imposing the boundary conditions (see Fig. 1). The nature of the  $T \rightarrow 0$  phase and its low energy spectrum of excited states is conveniently characterized by the superfluid density  $\rho_s$ , and the momentum ( $\vec{q}$ ) and imaginary time ( $\tau$ ) dependent correlation functions  $C_\rho(\vec{q}, \tau)$ ,  $C_K^{\alpha\alpha'}(\vec{q}, \tau)$  of local particle density and kinetic energy respectively ( $\alpha$  and  $\alpha'$  refer to the three possible bond orientations  $T_{0/1/2}$  shown in Fig. 1). We use standard SSE estimators<sup>18</sup> to calculate  $\rho_s$ ,  $C_\rho(\vec{q}, \tau = 0)$ ,  $S_\rho(\vec{q}, \omega_n = 0) = \int_0^\beta d\tau C_\rho(\vec{q}, \tau)$ ,  $C_K^{\alpha\beta}(\vec{q}, \tau = 0)$  and  $S_K^{\alpha\beta}(\vec{q}, \omega_n = 0) = \int_0^\beta d\tau C_K(\vec{q}, \tau)$ . These momentum space correlation functions are an unbiased probe of spatial order in the system. By analyzing the  $L$  and  $\beta$  dependence of the Bragg peaks at  $\pm\vec{Q} = \pm(2\pi/3, 2\pi/3)$  seen in the equal time and static correlation functions of density and kinetic energy, we conclude that spatial order

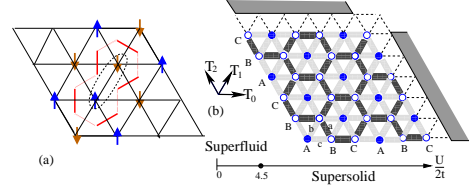


FIG. 1: a) A *flippable* pair of spins and the corresponding hexagon-pair with its flippable dimer configuration. Also shown are static spins that surround this flippable pair to form an elongated hexagonal tile. Tiling the lattice with these tiles gives a candidate insulating state at large  $U/t$  (not observed numerically). b) Actual  $T = 0$  phase diagram and nature of spatial symmetry breaking in the supersolid phase. Darker bonds and sites indicate higher kinetic energy and density respectively, and the state shown corresponds to  $\theta_K = \theta_n = 0$ . Note that the lattice is drawn to emphasize periodicity in directions  $T_0$  and  $T_2$ .

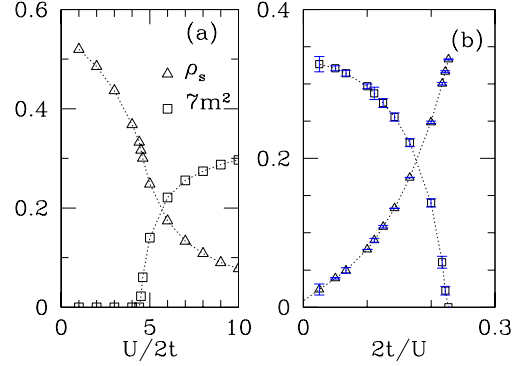


FIG. 2: Superfluid density  $\rho_s$  and density wave order parameter  $m^2 \equiv S_\rho(\vec{Q}, \omega_n = 0)/\beta L^2$  extrapolated to  $T \rightarrow 0$  and  $L \rightarrow \infty$ .

is established at these wavevectors when lattice translation symmetry is broken in the supersolid phase (in the convention used above, the components of  $\vec{Q}$  refer to projections in directions  $T_0$  and  $T_2$  shown in Fig. 1.)

We also measure two complex order parameters sensitive to this spatial symmetry breaking to obtain a better characterization of the supersolid state. These are defined as

$$\begin{aligned} \psi_n &= n_A + n_B e^{2\pi i/3} + n_C e^{4\pi i/3}, \\ \psi_K &= K_a + K_b e^{2\pi i/3} + K_c e^{4\pi i/3}. \end{aligned} \quad (2)$$

Here the subscripts refer to the three-sublattice decomposition of the triangular lattice into A, B, C type sites, and  $a \equiv BC$ ,  $b \equiv CA$ ,  $c \equiv AB$  type bonds respectively, while  $n$  and  $K$  are the densities and kinetic energies on the corresponding sites and bonds.  $\psi_K$  may be obtained from the Fourier components of the kinetic energies in the three lattice directions,  $K_{\vec{Q}}^{(0/1/2)}$ , using the relation  $\psi_K = e^{4\pi i/3} K_{\vec{Q}}^{(0)} + e^{2\pi i/3} K_{\vec{Q}}^{(1)} + e^{4\pi i/3} K_{\vec{Q}}^{(2)}$ , while  $\psi_n$  is precisely equal to  $n_{\vec{Q}}$ , the Fourier component of the

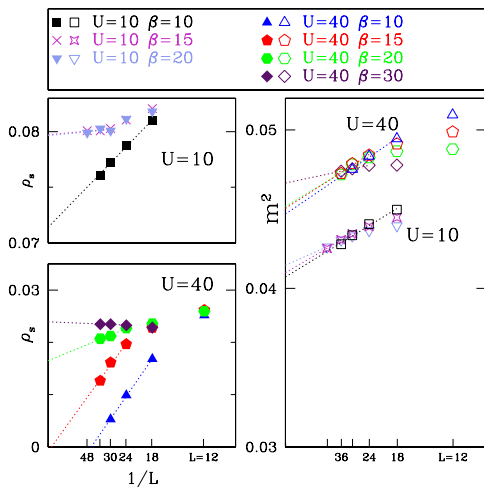


FIG. 3: Extrapolations implicit in Fig. 2 shown here for two values of  $U$

density at the ordering wavevector  $\vec{Q}$ . We expect both order parameters to average to zero as long as our algorithm remains ergodic—the probability distribution of their phases  $\theta_K$  and  $\theta_n$  however provides useful information regarding the nature of the supersolid phase.

*Numerical results:* Our numerical results for the variation in the superfluid density  $\rho_s$  as a function of  $U$  are shown in Fig. 2. Each point shown in Fig. 2 represents an extrapolation of available data to the  $T = 0$  thermodynamic limit. The results summarized in Fig. 2 show no indication of any finite  $U/t$  quantum phase transition beyond which  $\rho_s$  may become zero at zero temperature. Indeed, a smooth extrapolation of our data suggests that superfluidity persists in the low temperature limit at all finite values of  $U$ , albeit with an increasingly small  $T = 0$  value of  $\rho_s$ . While this is surprising from the perspective of putative Valence Bond Solid (VBS) ground states of the corresponding quantum dimer model, further insight can be obtained by performing a variational calculation using projected superfluid wavefunctions; this work will be reported separately.<sup>14</sup>

Although superfluidity survives in the entire range of  $U$  studied, the state at small  $U$  is not continuously connected to that at large  $U$ . Indeed, we see clear evidence for a continuous  $T = 0$  quantum phase transition at  $U_c \approx 4.45$ . This transition point is estimated using standard criteria in terms of Binder cumulants as shown in Fig. 4. (further details regarding the phase transition will be reported separately<sup>19</sup>). For  $U > U_c$ , the system spontaneously breaks lattice symmetry to produce a *supersolid* phase. To understand the nature of the supersolid phase, it is useful to analyze the joint probability distribution of the phases  $\theta_K$  and  $\theta_n$  defined earlier. At  $U = 10$ , we see from Fig. 5 that  $\theta_K$  is essentially pinned to be equal to  $-\theta_n$  (modulo  $2\pi$ ) at low temperature and large  $L$ , while  $\theta_n$  has a distribution which peaks at

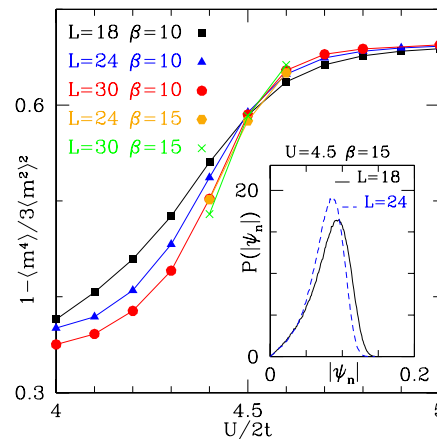


FIG. 4: Binder cumulant  $g = 1 - \langle m^4 \rangle / 3 \langle m^2 \rangle^2$  as a function of  $U$  in the transition region. From the location of the crossing point we identify a  $T = 0$  phase transition to the supersolid phase at  $U \approx 4.45$ . Inset: Histogram of  $|\psi_n|$  has a single peak, indicating a second-order transition

$\theta_n^p = 2\pi p/6$  with  $p$  an integer from 0 to 5. The picture that emerges (and gets sharper at larger  $L$  and  $\beta$ ) is thus of a state in which a relatively more mobile fluid of density  $\rho_{hx}$  living on a hexagonal lattice backbone of the full lattice is responsible for the superfluidity, while the centers of the hexagons have an average density of  $\rho_c$  that is less mobile. The six values of  $p$  correspond to three possible hexagonal backbones of a triangular lattice in conjunction with two choices for the sign of  $\rho_{hx} - \rho_c$ . Note that this spatial order is accompanied by a very slight deviation of the total density  $\rho$  from  $1/2$  (which survives in the  $T = 0$  thermodynamic limit), with the sign of deviation given by that of  $\rho_{hx} - \rho_c$ . We have also monitored these histograms at larger  $U \lesssim 40$ . We find that  $\theta_K$  remains strongly pinned to  $-\theta_n$ , and while the pinning of  $\theta_n$  and  $\theta_K$  individually does become weaker, the basic picture of the supersolid state remains the same.

*Landau theory:* Much of this picture of the supersolid phase can be understood within the framework of a Landau theory written in terms of the order parameters  $\psi_n$  and  $\psi_K$  (while it is not necessary to do so, we find it convenient to explicitly include  $\psi_K$  in our description). For our purposes here, it suffices to consider only the ‘potential energy’ terms of the Landau theory and leave out all fluctuation terms that involve spatial and time derivatives, or couplings to the superfluid order parameter, although these can also be straightforwardly written down. Terms in the Landau theory are constrained by the requirement of invariance under all the symmetries of the system. The action of these on our order parameters is simple to state: Under both lattice translations  $T_0$  and  $T_2$  we have  $\psi_n \rightarrow e^{2\pi i/3} \psi_n$ ,  $\psi_K \rightarrow e^{2\pi i/3} \psi_K$ , while under a  $\pi/3$  rotation about a  $A$  sublattice site, we have  $\psi_n \rightarrow \psi_n^*$ ,  $\psi_K \rightarrow \psi_K^*$ . Finally,  $\psi_n$  is odd under particle-hole transformations, while  $\psi_K$  is even. Terms consistent

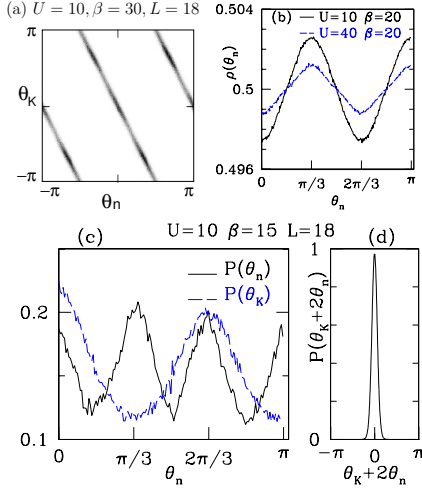


FIG. 5: Top panels: Greyscale plot of the joint probability distribution of  $\theta_n$  and  $\theta_K$ ;  $\theta_n$  dependence of  $\rho$ . Bottom panels: Probability distribution of  $\theta_n$ ,  $\theta_K + 2\theta_n$ , and  $\theta_K$ . The histogram of  $\theta_K + 2\theta_n$  has additional peaks at  $\pm 2\pi$  (not shown).

with these symmetries at  $\mu = 0$  give, up to sixth order

$$S_{pot}(\psi_n, \psi_K) = f(|\psi_n|^2, |\psi_K|^2) + c_{\theta n}(\psi_n^6 + \psi_n^{*6}) + c_{\theta K}(\psi_K^3 + \psi_K^{*3}) + c_{nK}(\psi_n^2 \psi_K + \psi_n^{*2} \psi_K^*). \quad (3)$$

As usual, spatial symmetry breaking corresponds to the function  $S_{pot}$  developing a minimum at a nonzero value of  $|\psi_n|$ . The detailed nature of the ordering is determined by the signs of coefficients  $c$  which fix the relative as well as absolute phases of the two order parameters. The results shown for  $U = 10$  in Fig. 5 can be modeled by taking all  $c$  negative, and this translates to the schematic picture of the phase shown in Fig. 1. In addition, the very slight  $\theta_n$  dependence of  $\rho - 1/2$  can be modeled<sup>23</sup> by the presence of a coupling term  $(\rho - 1/2)(\psi_n^3 + \psi_n^{*3})$  with a

tiny positive coefficient.

*Discussion:* We have thus established the presence of a persistent low-temperature supersolid phase on the triangular lattice. The remarkable stability of this phase is in contrast to the relatively small window of parameters within which supersolids have been previously seen on the square lattice.<sup>5,6</sup> Indeed, a smooth extrapolation of our data indicates that the supersolid phase persists in the  $U/t \rightarrow \infty$  limit. Our results thus throw up an interesting possibility for the observation of this phase in atom-trap experiments. It would therefore be useful to map out the finite temperature phase diagram for  $U > U_c$ . In the absence of any coupling between spatial and superfluid order parameters, superfluidity would be lost by a Kosterlitz Thouless (KT) phase transition, while crystalline order would be lost via two KT phase transitions with an intermediate power-law ordered crystal phase<sup>20</sup> analogous to that seen in the transverse field Ising antiferromagnet on the same lattice.<sup>21,22</sup> The coupling between the two order parameters is expected to modify the detailed nature of the finite temperature phase diagram; this will be reported on separately.<sup>19</sup> Our picture of the supersolid state indicates that it is not destabilized by doping, and this is currently under investigation.<sup>19</sup> Finally, it would also be interesting to study the stability of the supersolid upon relaxation of the hard-core constraint.

*Acknowledgements:* One of us (KD) would like to acknowledge stimulating discussions with A. Paramekanti and A. Vishwanath that led us to the work described here, and thank M. Barma, S. Gupta and T. Senthil for useful suggestions. We are also grateful to D. Dhar for very insightful suggestions, and M. Barma and D. Dhar for a critical reading of the manuscript. Computational resources of TIFR, and a student scholarship (DH) from the TIFR Alumni Fund are gratefully acknowledged. During completion of this work we became aware of parallel work<sup>23</sup> with similar conclusions, and would like to thank the authors, especially L. Balents, for correspondence comparing and contrasting our results.

- 
- <sup>1</sup> M. Greiner *et al.*, Nature **415** 39 (2002).
  - <sup>2</sup> L. M. Duan, E. Demler, and M. Lukin, Phys. Rev. Lett. **91**, 090402 (2003)
  - <sup>3</sup> L. Santos *et al.*, Phys. Rev. Lett. **93**, 030601 (2004)
  - <sup>4</sup> E. Kim and M. Chan, Nature **427**, 225 (2004); Science **305**, 1941 (2004).
  - <sup>5</sup> F. Hebert *et al.*, Phys. Rev. B **65**, 014513 (2002).
  - <sup>6</sup> P. Sengupta *et al.*, cond-mat/0412338, unpublished.
  - <sup>7</sup> E. Frey and L. Balents, Phys. Rev. B **55**, 1050 (1997).
  - <sup>8</sup> T. Senthil *et al.*, Science **303**, 1490 (2004); Phys. Rev. B **70**, 144407 (2004).
  - <sup>9</sup> R. Melko, A. Sandvik, and D. Scalapino, Phys. Rev. B **69**, 100408 (2004).
  - <sup>10</sup> A. Sandvik, S. Daul, R. Singh, and D. Scalapino, Phys. Rev. Lett. **89**, 247201 (2002).
  - <sup>11</sup> D. Jaksch *et al.*, Phys. Rev. Lett. **81**, 3108 (1998).
  - <sup>12</sup> S. Sachdev and M. Vojta, J. Phys. Soc. Japan, **69** Suppl. B, 1 (2000).
  - <sup>13</sup> R. Moessner, S. Sondhi, and P. Chandra, Phys. Rev. B **64**, 144416 (2001); Phys. Rev. Lett. **84**, 4457 (2000).
  - <sup>14</sup> K. Damle, D. Dhar, and D. Heidarian, unpublished.
  - <sup>15</sup> G. Murthy, D. Arovas, and A. Auerbach, Phys. Rev. B **55**, 3104 (1997).
  - <sup>16</sup> O. Syljuasen and A. Sandvik, Phys. Rev. E **66**, 046701 (2002)
  - <sup>17</sup> A. Sandvik, Phys. Rev. B **59**, R14157 (1999).
  - <sup>18</sup> A. Sandvik, J. Phys. A: Math. Gen. **25**, 3667 (1992).
  - <sup>19</sup> K. Damle and D. Heidarian, unpublished.
  - <sup>20</sup> J. Jose, L. Kadanoff, S. Kirkpatrick, and D. Nelson, Phys. Rev. B **16**, 1217 (1977).
  - <sup>21</sup> S. Isakov and R. Moessner, Phys. Rev. B **68**, 104409 (2003).
  - <sup>22</sup> D. Blankshtein, *et al.*, Phys. Rev. B **29**, 5250 (1984).
  - <sup>23</sup> R. Melko *et al.*, cond-mat/0505258 (unpublished).